Progress In Electromagnetics Research, PIER 83, 133–146, 2008

CPW-FED MULTI-BAND OMNI-DIRECTIONAL PLANAR MICROSTRIP ANTENNA USING COMPOSITE METAMATERIAL RESONATORS FOR WIRELESS COMMUNICATIONS

L.-M. Si and X. Lv

Department of Electronic Engineering
School of Information Science and Technology
Beijing Institute of Technology
Beijing 100081, P. R. China

Abstract—A novel approach for the design of a compact multi-band planar microstrip antenna is presented. This type of antenna is composed of composite metamaterial resonators (including conditional microstrip resonators and metamaterial resonators), and fed by signal feed. A sample antenna with composite closed-ring resonator and split-ring resonator (SRR) fed by 50 Ω coplanar waveguide (CPW) developed on FR4_epoxy substrate for multi-band wireless communication applications is presented. Appropriate design of the composite structure resulted in three discontinuous resonant bands. The fundamental magnetic resonant and electric resonant frequency of SRR and the first electric resonant frequency of the closed-ring resonator were combined to form low, middle, and high resonant band. The properties of this antenna are investigated by theoretical analysis and finite element method (FEM) simulations. The numerical results show that the proposed antenna has good impedance bandwidth and radiation characteristics in the three operating bands which cover the required band widths of the 2.4/5.2/5.8 GHz wireless local-area networks (WLAN) and 3.5/5.5 GHz worldwide interoperability for microwave access (WiMax) with return loss of better than 10 dB. The antenna also has stably omni-directional H-plane radiation patterns within the three operating bands.

1. INTRODUCTION

Metamaterial is artificial material that may exhibit electromagnetic (EM) responses not readily found in natural. In recent years, it has gained considerable attention since its unique EM characteristics can

be advantageous in design of novel EM components and devices [1–10]. One example is that the simultaneous effective negative permittivity ε and permeability μ feature of one type of metamaterials (called left-handed materials) can induce negative index of refraction, reversal of Doppler shift, and reversal of Cerenkov radiation phenomena [1–4]. It may be used for making perfect lens [5, 6], or even invisibility cloaks [7, 8]. Other examples are that electromagnetic/photonic band gap (EBG/PBG) and artificial magnetic metamaterial have already been used for antennas design, which might open the door to obtain the compact (sub-wavelength) and high performance EM components and devices [9, 10].

It is known that the negative permittivity can be obtained in the artificial plasmas (for instance, thin-wire structures) for all frequencies smaller than plasma frequency ω_P of plasmon medium due to $\varepsilon_{eff} = 1 - \frac{\omega_p^2}{\omega^2}$, where ε_{eff} is effective relative permittivity and ω is the frequency of incident EM wave [11, 12], but the negative permeability only occurs in a narrow magnetic resonant frequency band of artificial magnetic metamaterial resonators [13]. Split-ring resonator (SRR) is well-known artificial magnetic metamaterial and one of the essential components of left-handed material. The SRR consists of two concentric metal rings separated by a gap, each with a split at opposite sides. Though it was built up by nonmagnetic conductors (like copper), it can yield negative effective magnetic permeability, which was introduced by Pendry et al. in 1999 [13] and experimentally confirmed by Smith et al. in 2000 [2]. The EM behavior of SRR can be described as follows: when the incident EM wave frequency is tuned to the magnetic resonant frequency band the EM wave propagation represents a nearly totally transmittance in this metamaterial, but when the EM wave frequency out of the magnetic resonant frequency band (except the electric resonant frequency band of SRR which induced by the dipole-like charge distribution [14, 15]) the EM wave is nearly totally reflected. Naively, this feature of SRR may be used in EM engineering such as antennas, transmission lines system, frequency selective surfaces (FSSs), and filters for increasing their stop-band/pass-band characteristics.

Recently, antenna and its feed system in wireless communications require to be multifunctional for enhancing flexibility and feasibility, such as easy of integrate, low-profile, inexpensive and ease of fabrication, and wideband or multiband operating. Multiband antennas with frequency notched function are useful for wireless communications because a single antenna can cover several different frequency bands while decreasing noise interference at frequencies outside of the selected band [16]. In addition, coplanar waveguide

(CPW) transmission lines have been widely used for antenna feed system because its wide bandwidth, planar structures, and easy integration with monolithic microwave integrated circuits (MMIC) [16–18]. In order to design a multiband compact planar antenna with frequency notched function, we suggest that the antenna with CPW-fed is composed of different microstrip resonators, such as closed ring resonator and SRR, producing some discontinuous resonant bands.

In this paper, a sample antenna based on composite microstrip metamaterial resonators for multiband operation of wireless communications fed by 50 Ω CPW is proposed. The antenna has frequency notched function since the composite microstrip metamaterial resonators (closed-ring resonator and SRR) have three discontinuous resonant frequency bands. The operation bandwidth cover the required band widths of the IEEE 802.11 wireless local-area networks (WLAN) standards and worldwide interoperability for microwave access (WiMax) in the 2.4 GHz (2.4–2.484 GHz), 3.5 GHz (3.49–3.79 GHz), 5.2/5.5/5.8 GHz (5.15–5.35/5.25–5.85/5.725–5.825 GHz) have good impedance matching and radiation performance.

The paper is organized in the following sections. Section 2 contains the basic theory and the computational method. An effective finite element method (FEM) simulation tool is introduced in Section 3. Section 4 contains the modeling and simulations for different microstrip resonators and composite microstrip resonators antenna. The work is concluded in Section 5.

2. THEORY AND METHOD

Microstrip structure resonators have being used in a variety of systems as components of low-cost and low-profile antennas. All of resonators mentioned in this paper consist of microstrip structures. Figure 1 shows the schematic layout of different microstrip circular/ring resonators, such as circular disc resonator (Figure 1(a)), closed-ring resonator (Figure 1(b)), SRR (Figure 1(c)) and closed SRR (Figure 1(d)).

It is well known that the resonant frequencies of circular/ring resonators are determined by their dimensions, i.e., the resonant frequencies are generally directly proportional to their diameters. The relationship between resonant frequencies and diameters of these resonators has been studied with the equivalent circuit model method [19, 20] (also called "transmission-line model method" [13, 21–24]).

Following the early work of Watkins [23], the resonant frequencies and wavelengths of a circular disc resonator (Figure 1(a)) based on the

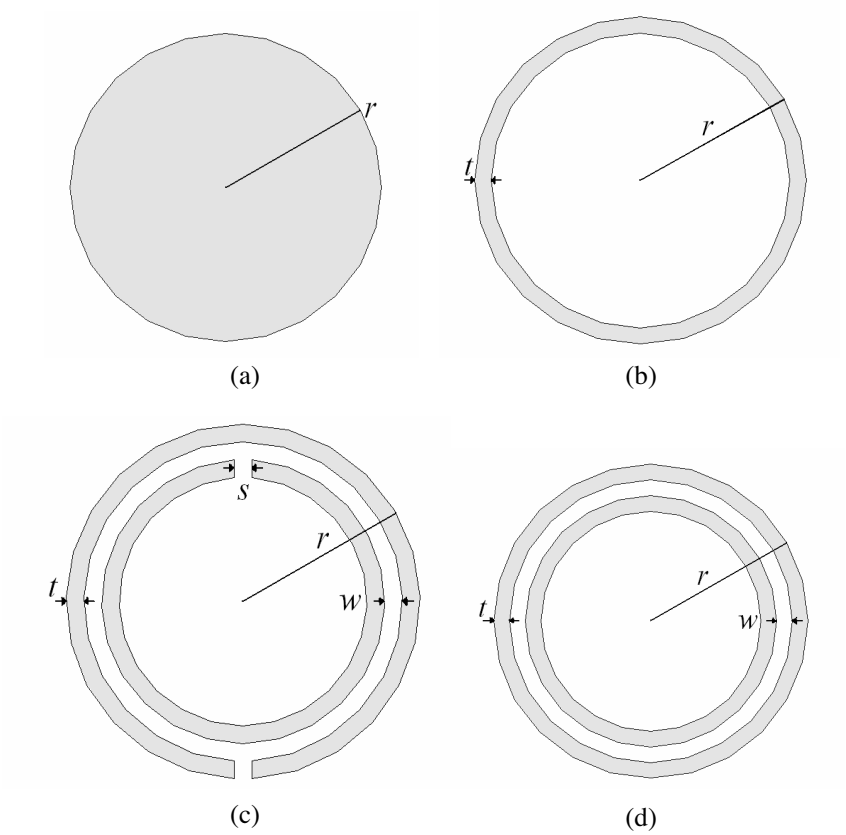

Figure 1. Layout configuration of (a) circular disc resonator, (b) closed-ring resonator, (c) SRR, and (d) closed SRR.

transmission-line model method are given by

$$f_{circular\_nm} = \frac{\alpha_{nm}}{2\pi r\sqrt{\varepsilon\mu}} = \frac{\alpha_{nm}c}{2\pi r\sqrt{\varepsilon_r\mu_r}} \tag{1a}$$

$$\lambda_{gcircular\_nm} = \frac{2\pi r}{\alpha_{nm}} \tag{1b}$$

where $f_{circular\_nm}$ is the resonant frequencies of circular disc resonator, $\lambda_{gcircular\_nm}$ is the corresponding guided wavelength, α_{nm} is the mth zero of the derivative of the Bessel function of order n, r is the radius of the circular disc resonator, c is the speed of light in free space, ε_r is the relative permittivity of substrate, and μ_r is the relative permeability of substrate which is equal to 1 for dielectric substrate (FR4_epoxy) in this paper. Therefore, the fundamental resonant frequency (i.e.,

the lowest order mode or the dominant mode) and its corresponding guided wavelength of the circular disc resonator are easily written as

$$f_{circular\_11} = \frac{1.841}{2\pi r\sqrt{\varepsilon\mu}} = \frac{1.841c}{2\pi r\sqrt{\varepsilon_r}} \tag{1c}$$

$$\lambda_{gcircular\_11} = \frac{2\pi r}{1.841} \tag{1d}$$

The resonant frequencies and guided wavelengths of a closed-ring resonator (Figure 1(b)) using transmission-line model method can be defined by [24]

$$f_{closed} = \frac{nc}{2\pi\sqrt{\varepsilon_r}r} \tag{2a}$$

$$\lambda_{gclosed} = \frac{2\pi r}{n} \tag{2b}$$

where f_{closed} is the resonant frequency of closed-ring resonator, $\lambda_{gclosed}$ (equal to $\lambda_0/\sqrt{\varepsilon_r}$) is the guided wavelength of closed-ring resonator, λ_0 is the wavelength in air, ε_r is relative permittivity of dielectric substrate, r is the radius of the closed-ring resonator, n is the mode number, ε_r is relative permittivity of dielectric substrate and c is the speed of light in free space.

The SRR (Figure 1(c)) is formed by two coupled conducting rings, i.e., two concentric metal rings separated by a gap, each with a split at opposite sides. Pendry and co-workers [13] calculated the fundamental magnetic resonant frequency of SRR also using the transmission-line model method given by

$$f_{SRR\_m} = \frac{c}{2\pi^2}\sqrt{\frac{3w}{\varepsilon_r(r-2t-w)^3}} \tag{3a}$$

$$\lambda_{gSRR\_m} = 2\pi^2\sqrt{\frac{(r-2t-w)^3}{3w}} \tag{3b}$$

where f_{SRR_m} is fundamental magnetic resonant frequency of SRR, λ_{gSRR_m} is the guided wavelength, ε_r is relative permittivity of dielectric substrate, r is the radius of the outer ring, t is the width of the metal lines, and w is the gap between the inner and outer ring. All parameters of the resonators are shown in Figure 1.

In addition, the SRR structure exhibits not only magnetic resonance but also electric resonance induced by the dipole-like charge distribution along the incident electric field. Aydin et al. have pointed out that closed SRR, i.e., the splits in the SRR are closed (see

Figure 1(d)), will destroy the magnetic resonance but still keep the electric resonance [14, 15]. Lots of experiments have demonstrated their predictions and shown that the first electric resonant frequency of SRR is higher than magnetic resonant frequency [14, 15].

Equivalent circuit model method [19, 20] (also called "transmission-line model method" [13, 21–24]) and EM full-wave simulation method are two key calculation methods used for composite metamaterials. For a composite metamaterial resonator using equivalent circuit model method, the energy loss corresponds to equivalent resistor, and the dielectrics and conductors represent the equivalent capacitance and inductance to create a resonant frequency band, that is, when a resonator is considered as a RLC circuit system the resonant frequency can be defined as $f_0 = \frac{1}{2\pi\sqrt{LC}}$. However, the EM full-wave simulation method based on finite element method (FEM), finite-difference time-domain (FDTD), or Method of Moment (MoM) is a more accurate and efficient method for metamaterials calculation, which will be discussed in the following Section.

3. FINITE ELEMENT METHOD (FEM) SIMULATION TOOL

Recently, EM full-wave simulations method has been widely used in the EM analysis of metamaterials. All of the EM full-wave simulation results were validated by comparison with experimental data and found to be in good agreement [2, 25–31]. EM full-wave simulations method, in principle, is usually much better than transmission-line model methods [13, 19–24]. It is because that the model methods based on simplified/quasi model can not consider the capacitive/inductive effects completely. EM full-wave simulation provided highly reliable method to analyze EM behavior of metamaterials, which has been supported by realistic structures and experimental data published previously [2, 25–31].

Ansoft commercial package High Frequency Structure Simulator (HFSS) [32] is a three-dimensional (3D) full-wave simulation software based on FEM. FEM is a powerful and efficient method for EM problems through subdividing a large problem into individually simple constituent units and then reassembling the solution for the entire problem space as a matrix of simultaneous equations [33]. FEM provides a numerical solution of Maxwell's equations, so HFSS as a powerful software is widely used for electromagnetic device design such as antennas, microwave filters, radio frequency integrated circuits (RFIC), waveguide components, and some other high frequency devices design.

There is a parameter optimization function in HFSS through automatically calculations and iterative solutions until a user-defined convergence criterion is met, which is suitable for fine-tune the device dimensions. Hence, HFSS can be used for EM simulations effectively.

4. MODELING AND SIMULATION

It is well-known that the CPW-fed antennas have advantages of wide bandwidth, planar structures, and easy integration with MMIC. CPW-fed antennas which are composed of different microstrip resonator and composite microstrip resonators are studied.

To acquire a small size antenna, the simulations of each of the four microstrip resonators (i.e., circular disc resonator, closed-ring resonator, SRR and closed SRR) with CPW-fed are carried out using HFSS. The relationships between their diameters ($2r$) and their fundamental resonances are tabulated in Table 1.

Table 1. The relationship between the diameters of the four CPW-fed resonators and fundamental resonances.

Fundamental resonant frequency f_0 (GHz)	Wavelength λ_0 at f_0 (mm)	Circular-dick resonator diameter $2r/\lambda_0$	Closed-ring resonator diameter $2r/\lambda_0$	SRR outer diameter $2r/\lambda_0$	Closed SRR outer diameter $2r/\lambda_0$
2.4	125	0.26	0.15	0.11	0.26
3.5	85.74	0.25	0.15	0.11	0.26
5.5	54.55	0.25	0.15	0.10	0.26

Table 1 demonstrated that the fundamental resonant frequency is determined by the diameter of each circular/ring microstrip resonators. The resonant frequency is directly proportional to their diameters, i.e., the fundamental resonant frequencies decrease with the increase of their diameters, which is list in Table 1. For instance, the diameter approximately corresponds to the quarter wavelength at fundamental resonant frequency for the circular disc. The wavelengths λ_0 of the fundamental magnetic resonant frequency and electric resonant frequency are about ten and four times of the outer diameter $2r$ of SRR, respectively. To overcome the classical half-wavelength size limitation and design antenna of very small dimension, an optimal design of an antenna with multi-band and frequency notched function may be consists of a closed-ring resonator and an SRR, because

the fundamental magnetic resonant frequency and electric resonant frequency of SRR and the fundamental electric resonant frequency of closed-ring resonator are combined to form low, middle, and high resonant band.

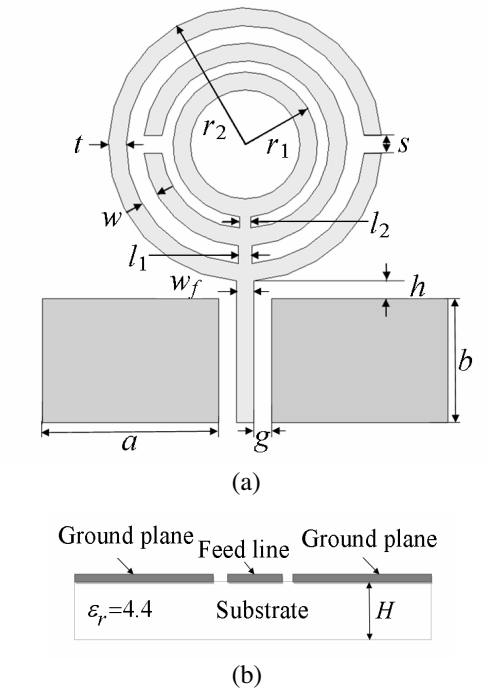

Figure 2. Structural configuration of the proposed antenna. (a) Top view; (b) Side view.

The configuration of the proposed antenna is shown in Figure 2. It consists of a closed-ring resonator and an SRR. The microstrip line of the resonators is fabricated with 0.018 mm-thick copper. The antenna is developed on an FR4_epoxy substrate with thickness $H = 0.8$ mm and relatively permittivity $\varepsilon_r = 4.4$. r_1 is the radius of the closed-ring resonator and r_2 is the radius of the outer ring of SRR. A 50 Ω CPW feed line, which has a width of the signal strip (free line) w_f fixed at 1 mm and a gap of distance between the strip and the coplanar ground plane g at 0.13 mm, is used to excite the proposed antenna. The spacing between the feed point and the ground plane is h. A tapered impedance transformer line has been applied for improving impedance matching. The width of the tapered transmission line at the feed point is w_f (equal to 1 mm), and the width of other tapered

transmission lines can be described as

$$l_n = 0.8^n \times w_f \quad (n = 1, 2) \tag{4}$$

To find the best radiation performance of the proposed antenna configurations, a parametric optimization was done by using HFSS. The antenna is designed to pass a specific resonant frequencies band with as small return loss as possible. Scattering parameter (S-parameter) is one of the general values to represent the performance of a microwave network. For an antenna, S-parameter S_{11} represents the relationship between the incoming wave (i) at excited port and the reflecting wave (r) at the same port defined as $r = S_{11} \times i$. Therefore, return loss of antenna is commonly specified by the S-parameter S_{11}. Figure 3 shows the calculated return loss (S_{11}) of the proposed antenna. The proper parameters for the proposed antenna configuration were: $r_1 = 4.1\,\text{mm}$, $r_2 = 7.75\,\text{mm}$, $t = 0.4\,\text{mm}$, $w = 1.1\,\text{mm}$, $s = 1\,\text{mm}$, $h = 0.4\,\text{mm}$, $w_f = 1\,\text{mm}$, $g = 0.13\,\text{mm}$, $a = 15\,\text{mm}$, $b = 10\,\text{mm}$, $H = 0.8\,\text{mm}$.

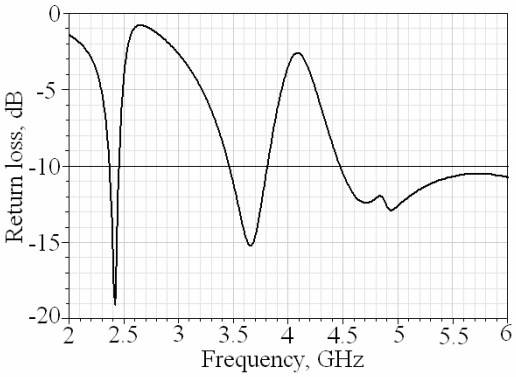

Figure 3. Return loss changes with frequency for proposed antenna with the parameters. $r_1 = 4.1\,\text{mm}$, $r_2 = 7.75\,\text{mm}$, $t = 0.4\,\text{mm}$, $w = 1.1\,\text{mm}$, $s = 1\,\text{mm}$, $h = 0.4\,\text{mm}$, $w_f = 1\,\text{mm}$, $g = 0.13\,\text{mm}$, $a = 15\,\text{mm}$, $b = 10\,\text{mm}$, and $H = 0.8\,\text{mm}$.

It can be seen that there are three resonant frequency bands: from 2.38 to 2.48, from 3.46 to 3.81, and from 4.50 to 6.00 GHz with return loss of better than 10 dB. They cover the required band widths of the IEEE 802.11 WLAN standards and WiMax in the 2.4 GHz (2.40–2.48 GHz), 3.5 GHz (3.49–3.79 GHz), 5.2/5.5/5.8 GHz (5.15–5.35/5.25–5.85/5.725–5.825 GHz).

The far-field radiation patterns in the E-plane and H-plane are shown in Figures 4(a)–(e) at 2.4, 3.5, 5.2, 5.5 and 5.8 GHz, respectively.

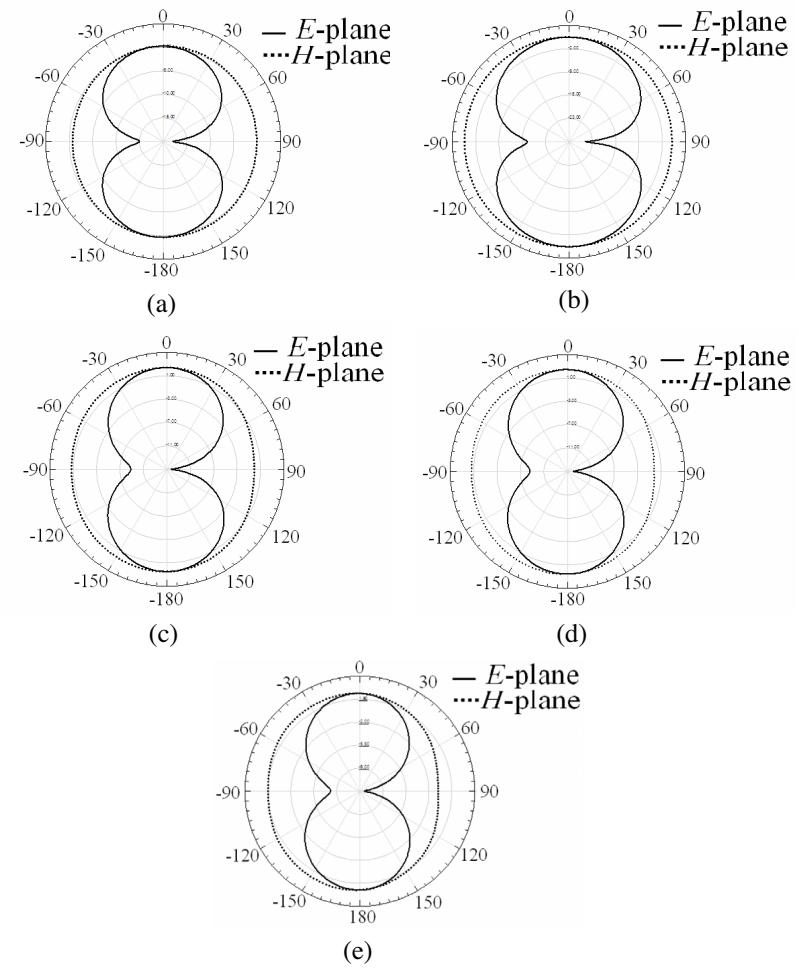

Figure 4. Radiation patterns in the E-plane (solid line) and H-plane (dotted line) of the proposed antenna at (a) 2.4 GHz, (b) 3.5 GHz, (c) 5.2 GHz, (d) 5.5 GHz and (e) 5.8 GHz.

As can be seen from Figure 4, the H-plane radiation patterns of the proposed antenna are stably omni-directional. The antenna gain is about 0.3∼0.5 dB in the low-band (2.38–2.48 GHz), 1.5∼1.7 dB in the middle-band (3.46–3.81 GHz), and 2.5∼3.2 dB in the high-band (4.5–6 GHz). Therefore, the proposed antenna is planar, small size, and suitable for WLAN and WiMax applications. The antenna occupies a circular area with radius of 7.75 mm on a printed circuit board which

has overcome half-wavelength size limitation and further improved to utilize the triband in WLAN/WiMax applications.

5. CONCLUSION

A new compact and planar multiband antenna with composite microstrip metamaterial resonators has been presented. The antenna is suitable for multi-band mobile devices and offers advantages in small size, planar, inexpensive and ease to manufacture, omni-directional H-plane radiation patterns, and good radiation performance. A sample antenna with frequency notched function is proposed for triband WLAN/WiMax wireless communications applications. By using composite closed-ring resonator and SRR to produce three discontinue resonant frequency bands, the antenna is suitable for WLAN/WiMax (2.4/3.5/5.2/5.5/5.8 GHz) wireless communication. To improve impedance bandwidth and impedance matching, the antenna is fed by 50 Ω CPW and tapered impedance transformer line. The numerical results show that the proposed antenna with small size and planar structure has proper impedance bandwidth covering the required band widths of WLAN and WiMax in the 2.4–2.484 GHz, 3.49–3.79 GHz, and 5.15–5.825 GHz and stably omni-directional H-plane radiation patterns.

REFERENCES

1. Veselago, V. G., "The electrodynamics of substances with simultaneously negative values of ε and μ," *Soviet Physics Uspekhi*, Vol. 10, No. 4, 509–514, 1968.
2. Smith, D. R., J. P. Willie, D. C. Vier, S. C. Nemat-Nasser, and S. Schultz, "Composite medium with simultaneously negative permeability and permittivity," *Physical Review Letters*, Vol. 84, 4184–4187, 2000.
3. Chen, H., B. I. Wu, and J. A. Kong, "Review of electromagnetic theory in left-handed materials," *Journal of Electromagnetic Waves and Applications*, Vol. 20, No. 15, 2137–2151, 2006.
4. Kong, J. A., "Electromagnetic wave interaction with stratified negative isotropic media," *Progress In Electromagnetics Research*, PIER 35, 1–52, 2002.
5. Pendry, J. B., "Negative refraction makes a perfect lens," *Physical Review Letters*, Vol. 85, 3966–3969, 2000.
6. Srivatava, S. K. and S. P. Ojha, "Enhancement of omnidirectional reflection bands in one-dimensional photonic crystals with

left-handed materials," *Progress In Electromagnetics Research*, PIER 68, 91–111, 2007.

7. Schurig, D., J. J. Mock, B. J. Justice, S. A. Cummer, J. B. Pendry, A. F. Starr, and D. R. Smith, "Metamaterial electromagnetic cloak at microwave frequencies," *Science*, Vol. 314, Vol. 58010, 977–980, 2006.
8. Fu, Y. Q, Q. R. Zhang, Q. Gao, and G. H. Zhang, "Mutual coupling reduction between large antenna arrays using electromagnetic bandgap (EBG) structures," *Journal of Electromagnetic Waves and Applications*, Vol. 20, No. 6, 819–825, 2006.
9. Pirhadi, A., M. Hakkak, and F. Keshmiri, "Using electromagnetic bandgap superstrate to enhance the bandwidth of probe-fed microstrip antenna," *Progress In Electromagnetics Research*, PIER 61, 215–230, 2006.
10. Nader, E. and R. W. Ziolkowski, "A positive future for double-negative metamaterials," *IEEE Transactions on Microwave Theory and Techniques*, Vol. 53, No. 4, 1535–1556, 2005.
11. Pendry, J. B., A. J. Holden, W. J. Stewart, and I. Youngs, "Extremely low frequency plasmons in metallic mesostructures," *Physical Review Letters*, Vol. 76, 4773–4776, 1996.
12. Pendry, J. B., A. J. Holden, D. J. Robbins, and W. J. Stewart, "Low frequency plasmons in thin-wire structures," *Journal of Physics: Condensed Matter*, Vol. 10, 4785–4809, 1998.
13. Pendry, J. B., A. J. Holden, D. J. Robins, and W. J. Stewart, "Magnetism from conductors and enhanced nonlinear phenomena," *IEEE Transactions on Microwave Theory and Techniques*, Vol. 47, 2075–2084, 1999.
14. Koschny, T., M. Kafesaki, E. N. Economou, and C. M. Soukoulis, "Effective medium theory of left-handed materials," *Physical Review Letters*, Vol. 93, 107402, 2004.
15. Su, S. W., K. L. Wong, and F. S. Chang, "Compact printed ultra-wideband slot antenna with a band-notched operation," *Microwave and Optical Technology Letters*, Vol. 54, No. 2, 128–130, 2005.
16. Kim, Y. and D. H. Kwon, "CPW-fed planar ultra wideband antenna having a frequency band notch function," *Electronics Letters*, Vol. 40, No. 7, 403–405, 2004.
17. Liu, W. C. and C. F., Hsu, "CPW-fed notched monopole antenna for UMTS/IMT-200/WLAN applications," *Journal of Electromagnetic Waves and Applications*, Vol. 21, No. 6, 841–851,

2007.

18. Liu, W. C. and H. J. Liu, "Miniaturized asymmetrical CPW-fed meandered strip antenna for triple-band operation," *Journal of Electromagnetic Waves and Applications*, Vol. 21, No. 8, 1089–1097, 2007.
19. Wu, B., B. Li, T. Su, and C. H. Liang, "Equivalent-circuit analysis and low pass filter design of split-ring resonator DGS," *Journal of Electromagnetic Waves and Applications*, Vol. 20, No. 14, 1943–1953, 2006.
20. Li, D., Y. J. Xie, P. Wang, and R. Yang, "Applications of split-ring resonances on multi-band frequency selective surfaces," *Journal of Electromagnetic Waves and Applications*, Vol. 21, No. 11, 1551–1563, 2007.
21. Xu, W., L. W. Li, H. Y. Yao, and T. S. Yeo, "Extraction of constitutive relation tensor parameters of SRR structures using transmission line theory," *Journal of Electromagnetic Waves and Applications*, Vol. 20, No. 1, 13–25, 2006.
22. Chen, H., L. Ran, B. I. Wu, J. A. Kong, and T. M. Grzegorczyk, "Crankled S-ring resonator with small electrical size," *Progress In Electromagnetics Research*, PIER 66, 179–190, 2006.
23. Watkins, J., "Circular resonant structures in microstrip," *Electronics Letters*, Vol. 5, No. 21, 524–524, 1969.
24. Chang, K., *Microwave Ring Circuits and Antennas*, Wiley, New York, 1996.
25. Lin, X. Q., Q. Cheng, R. P. Liu, D, Bao, and T. J. Cui, "Compact resonator filters and power dividers designed with simplified meta-structures," *Journal of Electromagnetic Waves and Applications*, Vol. 21, No. 12, 1663–1672, 2007.
26. Aydin, K., K. Guven, M. Kafesaki, L. Zhang, and C. M. Soukoulis, "Experimental observation of true left-handed transmission peaks in metamaterials," *Optics Letters*, Vol. 29, No. 22, 2623–2635, 2004.
27. Yang, R., Y. Xie, P. Wang, and L. Li, "Microstrip antennas with left-handed materials substrates," *Journal of Electromagnetic Waves and Applications*, Vol. 20, No. 9, 1943–1953, 2006.
28. Xu, W., L. W. Li, H. Y. Yao, and Q. Wu, "Left-handed material effects on waves modes and resonant frequencies: Filled waveguide structures and substrate-loaded patch antennas," *Journal of Electromagnetic Waves and Applications*, Vol. 19, No. 15, 2033–2047, 2005.
29. Grzegorczyk, T. M. and J. A. Kong, "Review of left-handed

metamaterials: Evolution from theoretical and numerical studies to potential applications," *Journal of Electromagnetic waves and Applications*, Vol. 20, No. 14, 2053–2064, 2006.

30. Yang, R., Y. Xie, D. Li, J. Zhang, and J. Jiang, "Bandwidth enhancement of microstrip antennas with metamaterial bilayered substrated," *Journal of Electromagnetic waves and Applications*, Vol. 21, No. 15, 2321–2330, 2007.
31. Guo, Y. and R. Xu, "Planar metamaterials supporting multiple left-handed modes," *Progress In Electromagnetics Research*, PIER 66, 239–251, 2006.
32. HFSS, Ansoft Software Inc., USA.
33. Jin, J. M., *The Finite Element Method in Electromagnetics*, 2nd edition, Wiley-IEEE Press, 2002.